Separation Science and Technology
Publication details, including instructions for authors and subscription information:
http://www.informaworld.com/smpp/title~content=t713708471

Extraction of Phenol and Cresol by Liquid Surfactant Membrane

Masaaki Teramoto[a]; Hiroshi Takihana[a]; Michiru Shibutani[a]; Takahiro Yuasa[a]; Naotake Hara[a]
[a] DEPARTMENT OF INDUSTRIAL CHEMISTRY, KYOTO INSTITUTE OF TECHNOLOGY MATSUGASAKI, KYOTO, JAPAN

To cite this Article Teramoto, Masaaki , Takihana, Hiroshi , Shibutani, Michiru , Yuasa, Takahiro and Hara, Naotake(1983) 'Extraction of Phenol and Cresol by Liquid Surfactant Membrane', Separation Science and Technology, 18: 5, 397 — 419
To link to this Article: DOI: 10.1080/01496398308060284
URL: http://dx.doi.org/10.1080/01496398308060284

SEPARATION SCIENCE AND TECHNOLOGY, 18(5), pp. 397–419, 1983

Extraction of Phenol and Cresol by Liquid Surfactant Membrane

MASAAKI TERAMOTO,* HIROSHI TAKIHANA,
MICHIRU SHIBUTANI, TAKAHIRO YUASA,
and NAOTAKE HARA

DEPARTMENT OF INDUSTRIAL CHEMISTRY
KYOTO INSTITUTE OF TECHNOLOGY
MATSUGASAKI, SAKYO-KU, KYOTO 606, JAPAN

Abstract

A model for the extraction of weak acids or weak bases by means of liquid surfactant membranes is presented in which external mass transfer around W/O emulsion drop, internal mass transfer inside W/O emulsion drop, both phase and chemical equilibria, and the drop size distribution of W/O emulsion are taken into account. The experimental results on the batch extraction of phenol, *o*- and *p*-cresol are found to be satisfactorily simulated by the proposed model. The effect of the intensity of sonication in the preparation of W/O emulsion on the extraction rate is also presented.

INTRODUCTION

The separation method by liquid surfactant membranes has been noted as a new technique for the separation of hydrocarbons (*1–8*) and the removal and/or the recovery of various compounds such as phenol (*9–11*), amines (*12–13*), and heavy metals (*12, 14–21*).

While a number of investigators have experimentally demonstrated that liquid surfactant membranes are useful for separating various materials, very few studies have been presented on the mechanism and the mathematical model of solute permeation. Cahn and Li (*10*) presented a very simplified model for the extraction of phenol which assumed that the extraction rate is

---

*To whom correspondence should be addressed.

0149-6395/83/1805-0397$3.50/0

proportional to the solute concentration difference between two aqueous phases. Later, Matulevicius and Li (*15*), Völkel et al. (*19*), and Kremesec (*8*) proposed a model in which mass transfer resistance is localized in the peripheral oil or water layer of the emulsion drop, and the complete mixing inside the drop is assumed. It is evident, however, that this model cannot be applied to the case where the internal mass transfer resistance is controlling. Casamatta et al. (5) analyzed the permeation rate of hydrocarbons through water membranes in an O/W/O emulsion system by taking mass transfer resistances both inside and outside the O/W emulsion drop into account, and found that the diffusion through the peripheral water layer of the O/W emulsion drop is rate controlling because of very low solubility of hydrocarbons in water phase. Recently, Ho et al. (*11*) proposed a shrinking core model for the extraction of phenol. However, in this model the external mass transfer resistance around the W/O emulsion drop, which might be more important than the internal resistance in the early stage of the extraction, was neglected. Furthermore, because chemical equilibria in the internal aqueous phase containing NaOH and phenol were not considered, this model cannot predict the equilibrium concentration of phenol attained when three phases, i.e., the internal and external aqueous phases and the oil membrane phase, are in equilibrium.

The present authors (*13*) presented a mass transfer model for the extraction of amine and phenol by liquid surfactant membranes in which the diffusion in the W/O emulsion drops, the external mass transfer, and both

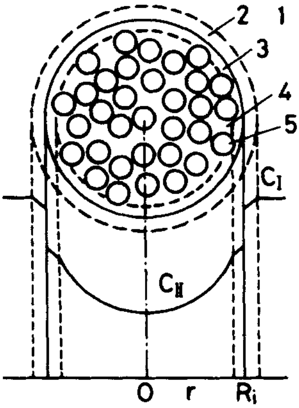

FIG. 1. Schematic diagram of W/O/W multiphase emulsion system. 1: External aqueous phase (Phase I). 2: Film of Phase I around W/O emulsion drop. 3: Peripheral oil layer. 4: Oil phase (Phase II). 5: Internal aqueous phase (Phase III).

phase and chemical equilibria were taken into account. It was shown that the effects of various experimental conditions on the rate of the extraction of aniline could be successfully explained by the model. However, the uniform size of the W/O emulsion drop was assumed in that model.

In this paper a modified mass transfer model is presented in which the drop size distribution of the W/O emulsion is taken into account. Furthermore, the extraction of phenol, *o*-, and *m*-cresol was carried out using a W/O/W multiphase emulsion which consists of an external aqueous phase containing phenol (Phase I), internal droplets of an aqueous NaOH or LiOH solution (Phase III), and an oil membrane phase (Phase II) as shown in Fig. 1. The experimental data are analyzed on the basis of the present model. The effect of the preparation method of the W/O emulsion on its properties and the extraction rate is also presented.

THEORY

Chemical Equilibria

We consider the case where phenol dissolves in an aqueous solution containing NaOH or LiOH. Dissociation equilibria of phenol and water are expressed by Eqs. (1) and (2), respectively.

$$K_a = [\mathrm{PhO^-}][\mathrm{H^+}]/[\mathrm{PhOH}] = P[\mathrm{H^+}]/C \qquad (1)$$

$$K_w = [\mathrm{H^+}][\mathrm{OH^-}] \qquad (2)$$

The charge balance equation is

$$[\mathrm{M^+}] + [\mathrm{H^+}] = [\mathrm{PhO^-}] + [\mathrm{OH^-}], \ (A + [\mathrm{H^+}] = P + [\mathrm{OH^-}]) \quad (3)$$

where M is Na or Li, A is the concentration of $\mathrm{OH^-}$, C and P are the concentrations of phenol and phenolate ion, respectively, and K_a and K_w are the acid dissociation constant of phenol and the ion product of water, respectively. Phenol exists in both undissociated and dissociated forms. Then T, the total concentration, is given by

$$[\mathrm{PhOH}]_T = [\mathrm{PhOH}] + [\mathrm{PhO^-}], \qquad T = C + P \qquad (4)$$

$[\mathrm{H^+}]$ is much less than $[\mathrm{OH^-}]$ in the internal aqueous phase. Then, Eq. (5) is derived from Eqs. (1)–(4):

$$T = C\{(A + C)K_a + K_w\}/(K_a C + K_w) \tag{5}$$

On the other hand, phenol exists in the undissociated form in the external aqueous phase because its pH is maintained much lower than pK_a of phenol.

Mass Transfer Model

Here, the previous model is extended to the case where the drop size distribution of the W/O emulsion exists. Hereafter the "drop" refers to the W/O emulsion drop dispersed in Phase I, and the "droplet" the internal drop in the W/O emulsion drop. If the number and the volume fraction of the drops of radius R_i in the system are n_i and ϕ'_i, respectively, the following equation holds.

$$\phi'_i = (4/3)\pi n_i R_i^3 / V_T, \qquad i = 1 - N \tag{6}$$

Here, V_T is the total volume of the system and N is the number of divisions of the drop size distribution. The mass balance equation of phenol in the external aqueous phase is represented by

$$-(1 - \phi')\frac{\partial C_I}{\partial t} = \sum_{i=1}^{N} \frac{3\phi'_i}{R_i} K_0\{C_\mathrm{I} - (C_{\mathrm{II},i})_{r=R_i}/K\} \tag{7}$$

where C_I is the solute concentration in the external phase, K is the partition coefficient defined by $(C_\mathrm{II}/C_I)_\mathrm{eq}$, ϕ' is the volume fraction of W/O emulsion phase ($= (V_\mathrm{II} + V_\mathrm{III})/V_\mathrm{T}$), and K_0 is the overall mass transfer coefficient through the external boundary layer of aqueous phase around the W/O emulsion drop and the peripheral oil layer of the drop. V_I, V_II, and V_III are the volumes of the external phase, the membrane phase, and the internal phase, respectively. The diffusion equation in the drop is

$$(1 - \phi)\frac{\partial C_{\mathrm{II},i}}{\partial t} + \phi\frac{\partial T_{\mathrm{III},i}}{\partial t} = D_e\left(\frac{\partial^2 C_{\mathrm{II},i}}{\partial r^2} + \frac{2}{r}\frac{\partial C_{\mathrm{II},i}}{\partial r}\right) \tag{8}$$

where T_III is the total concentration of phenol in the internal phase, D_e is the effective diffusivity in the W/O emulsion phase, and ϕ is $V_\mathrm{III}/(V_\mathrm{II} + V_\mathrm{III})$. Here, the equilibrium between the oil and the internal aqueous phases is assumed (*13*). The initial and the boundary conditions are expressed as follows:

$$\text{I.C.:}\quad C_I = C_{I,0},\quad C_{II,i} = 0 \text{ for } 0 \leq r \leq R_i,\ t = 0 \tag{9}$$

$$\text{B.C.1:}\quad \partial C_{II,i}/\partial r = 0 \text{ at } r = 0,\ t \geq 0 \tag{10}$$

$$\text{B.C.2:}\quad K_0\{C_I - (C_{II,i})_{R_i}/K\} = D_e(\partial c_{II,i}/\partial r)_{R_i} \text{ at } r = R_i,\ t \geq 0 \tag{11}$$

Here it is assumed that the thickness of the peripheral oil layer is negligibly small compared to the radius of the W/O emulsion drop.

The above equations are transformed into dimensionless form by using variables and parameters expressed by Eq. (18):

$$-\partial y_I/\partial\theta = 3Bi_C(1-\phi')\sum_{i=1}^{N}(\phi_i' R_C/R_i)\{y_I - (y_{II,i})_{x=1}\} \tag{12}$$

$$\frac{\partial y_{II,i}}{\partial\theta} = \frac{(R_C/R_i)^2}{1-\phi+(\phi/K)g(y_{II,i})}\left(\frac{\partial^2 y_{II,i}}{\partial x^2} + \frac{2}{x}\frac{\partial y_{II,i}}{\partial x}\right) \tag{13}$$

$$\text{I.C.:}\quad y_I = 1,\quad y_{II,i} = 0 \text{ for } 0 \leq x \leq 1,\ \theta = 0 \tag{14}$$

$$\text{B.C.1:}\quad \partial y_{II,i}/\partial x = 0 \text{ at } x = 0,\ \theta \geq 0 \tag{15}$$

$$\text{B.C.2:}\quad (\partial y_{II,i}/\partial x)_{x=1} = (Bi_C/K)(R_i/R_C)\{y_I - (y_{II,i})_{x=1}\} \text{ at } x = 1,\ \theta \geq 0 \tag{16}$$

where $g(y_{II,i})$ in Eq. (13) is given by Eq. (17):

$$g(y_{II,i}) = dT_{III,i}/dC_{III} = 1 + \alpha\beta/(y_{II,i}+\alpha)^2 \tag{17}$$

$$\left.\begin{aligned} &x = r/R_i,\ y_I = C_I/C_{I,0},\ y_{II,i} = C_{II,i}/KC_{I,0},\ \theta = D_e t/R_C^2 \\ &Bi_C = K_0R_C/D_e,\ \alpha = K_w/K_aC_{I,0},\ \beta = A_0/C_{I,0} \end{aligned}\right\} \tag{18}$$

If the six parameters ϕ, ϕ', K, α, β, and Bi_C and the drop size distribution are given, the basic equations can be numerically solved. Here R_C is the characteristic radius of the drop, and is taken as 0.05 cm in this study. The finite difference method was used to solve the basic equations.

EXPERIMENTAL

The experimental apparatus and the procedure were the same as reported in a previous paper (*13*) except the methods of the preparation of W/O emulsion and the measurement of the rate of the leakage of the internal aqueous phase to the external phase.

The W/O emulsion was prepared as follows. A mixture of 50 cm^3 of kerosene containing 5 vol% of Span 80 (sorbitan monooleate) and the same volume of aqueous solution of NaOH or LiOH was agitated for 15 min by a vibromixer. Then the mixture was sonicated by an ultrasonic homogenizer (Nippon Seiki Ltd., US-150W) by either the direct or indirect method as shown in Fig. 2. In the direct method the tip of the homogenizer was immersed in the solution. In this case much smaller droplets were obtained due to the high intensity of sonication than in the case of indirect sonication. The W/O emulsion thus prepared was added to an agitation vessel containing 550 cm^3 of deionized water under stirring at 188 rpm. The vessel was 9 cm in inner diameter, and equipped with a six-bladed turbine agitator. In about 2 min, phenol solution was poured into the vessel to start extraction. The total volume was 750 cm^3.

The partition coefficient of phenol between kerosene and water was measured by shaking the two phases and analyzing for the phenol concentration in the aqueous phase with a spectrophotometer (Shimadzu UV 200S). However, when Span 80 was added to kerosene, the aqueous and oil phases were emulsified by shaking, and the two phases could not be separated. This problem was overcome by using a W/O/W emulsion system, i.e., physical extraction of phenol into W/O emulsion drops was carried out without adding LiOH to the internal aqueous phase, and after equilibration the external and emulsion phases were easily separated by settling, and phenol in the external phase was analyzed.

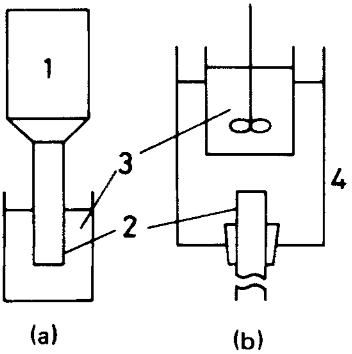

FIG. 2. Method of sonication. (a) Direct sonication. (b) Indirect sonication. 1: Ultrasonicator. 2: Tip of ultrasonicator. 3: W/O emulsion. 4: Water bath.

The fraction of the leakage of the internal aqueous phase to the external phase due to the breakage of oil membrane was determined by analyzing the concentration of Li, which was initially present only in the internal phase, in the external phase by a flame emission spectrophotometer (Nippon Jarrel Ash atomic absorption and flame emission spectrophotometer, AA-782). The fraction of leakage, f, was calculated by

$$f = (1 - \phi')[\mathrm{Li}^+]_\mathrm{I}/(\phi\phi'[\mathrm{Li}^+]_{\mathrm{III},0}) \tag{19}$$

Because Na is contained in Span 80 and it dissolves in water when the oil phase is contacted with water, Na cannot be used as a tracer for the measurement of f.

The viscosity of the W/O emulsion and the interfacial tension between aqueous and emulsion phases were measured with a cone-and-plate viscometer (Tokyo Seiki Ltd., Visconic ED), and a Wilhelmy plate surface tensiometer (Kyowa Kagaku Ltd., A-3), respectively. The drop size distribution of the W/O emulsion was measured by the photographic method, and the internal droplets were inspected by the microscopic method. The temperature was 298 K.

RESULTS

Partition Coefficient

Figure 3 shows the effect of the concentration of Span 80 on K, the partition coefficients of phenol and *o*- and *p*-cresol. K increases with increasing [Span 80] probably because the polarity of the oil phase increases by adding a polar compound such as Span 80 to kerosene. It is important to recognize that the surfactant serves to stabilize the emulsion as well as to increase the solubility of solute in the membrane.

Effect of Method of Sonication

Four ways of the preparation of W/O emulsion were attempted by changing the method and the time of sonication:

(A) Direct sonication, 1 min
(B) Direct sonication, 30 s
(C) Indirect sonication, 22 min
(D) Indirect sonication, 10 min

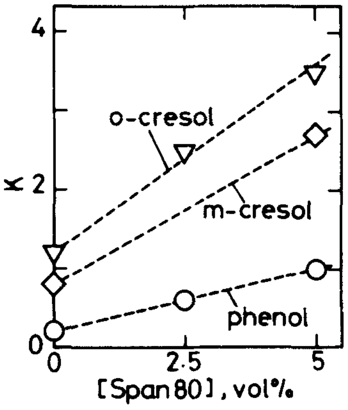

FIG. 3. Effect of the concentration of Span 80 on the partition coefficients of phenol and cresol.

The properties of the emulsion thus obtained are summarized in Table 1. The intensity of sonication decreased in the order of A > B > C > D. Thus the size of the droplet increased, and the interfacial area between the oil and the internal aqueous phases decreased in the same order. In the case of C and D, the interface was probably saturated by the adsorbed layer of Span 80, and the surface tension was low. On the other hand, in the case of A, the amount of Span 80 was insufficient to saturate the interface, which resulted in relatively high interfacial tension. The interfacial tension between oil phases containing various amount of Span 80 and aqueous phase is shown in Fig. 4. It is recognized from the values of the interfacial tension shown in

TABLE 1
Effect of Intensity of Sonication in Preparation of W/O Emulsion

Condition of sonication	Diameter of internal droplet R_μ (μm)	Apparent viscosity[a] η (Pa·s)	Interfacial tension σ (N/m)	Sauter mean diameter of W/O emulsion drop d_{32} (mm)	Fraction of leakage of Phase II,[b] f
Method A	<1	0.0289	0.021	1.52	0.0180
Method C	1–3	0.0265	0.016	1.02	0.0177
Method D	1–7	0.0221	0.0105	0.82	0.0219

[a] Values at the shear rate of 38.4 s^{-1}.
[b] Values at $t = 15$ min.

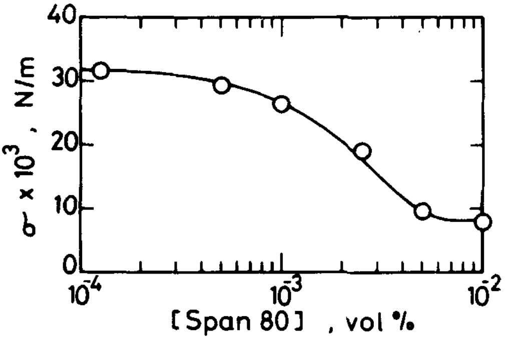

FIG. 4. Effect of the concentration of Span 80 on the interfacial tension of water–kerosene system.

Table 1 and Fig. 4 that the bulk concentration of Span 80 in oil for intensive sonication is as low as 0.002 vol%, and most of the surfactant added to the oil is adsorbed at the interface. The apparent viscosity of the emulsion increased as the diameter of the internal droplet became small, in accordance with the previous results (*22*).

The distribution of the size of the W/O emulsion drops dispersed in the external aqueous phase under the same stirring condition is shown in Fig. 5. It is seen that the diameter became large with an increase in the intensity of sonication. The plot of Sauter mean diameter of the W/O emulsion drop vs interfacial tension is shown in Fig. 6. The slope is about 0.8, and is greater than 0.6, the value reported for many liquid–liquid dispersions (*23, 24*). This deviation may be due to the increase in emulsion viscosity with the intensity of sonication.

The effect of the preparation method of W/O emulsion on the extraction rate of phenol is shown in Fig. 7, which indicates that the rate decreased with increasing sonication intensity because of the formation of large drops.

Effect of Initial Concentration of Phenol

As shown in Fig. 8, the higher the initial concentration of phenol, $C_{t,0}$, the lower the extent of extraction. This is because the internal droplets in the peripheral region of the drops are more rapidly saturated with phenol when

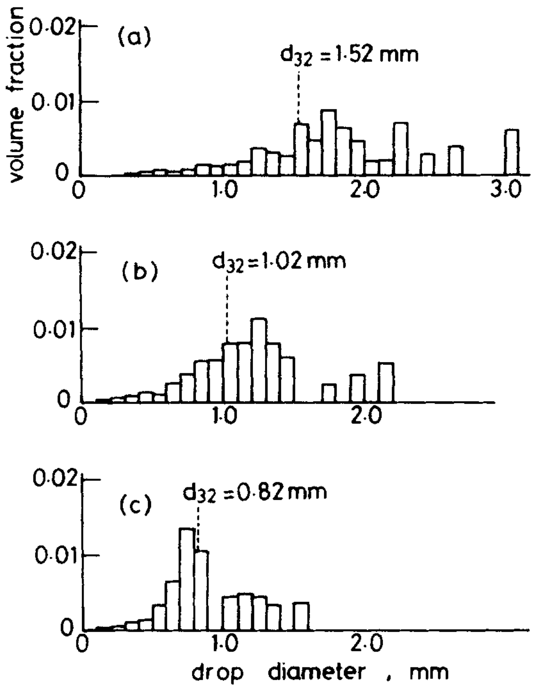

FIG. 5. Drop size distribution of W/O emulsion. (a) Method A. (b) Method C. (c) Method D.

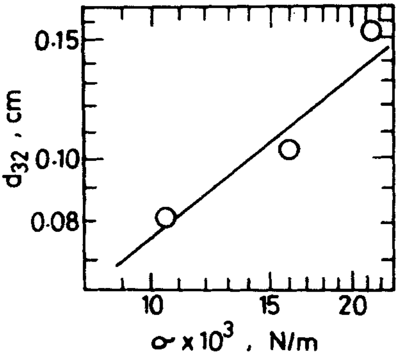

FIG. 6. Plot of Sauter mean diameter of W/O emulsion drop vs interfacial tension.

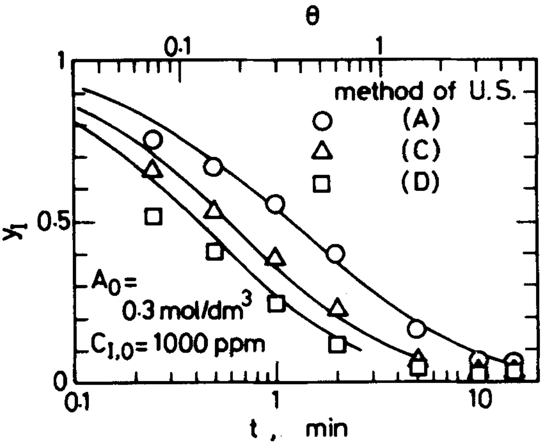

FIG. 7. Effect of the method of sonication on the extraction rate of phenol. Solid lines are the calculated results ($D_e = 1.26 \times 10^{-5}$ cm^2/s, $K_0 = 0.0038$ cm/s).

$C_{I,0}$ is higher. Comparison of Fig. 8(a) with 8(b) indicates that in the former case, the drop size is larger, and the effect of $C_{I,0}$ is more remarkable than in the latter case, suggesting that internal mass transfer resistance is important.

Effect of Concentration of Sodium Hydroxide

In Fig. 9 is shown the effect of initial sodium hydroxide concentration A_0 on the extraction rate. The rate increased with an increase in NaOH concentration because of a higher capacity for trapping phenol in the internal phase. However, this effect was not remarkable because the drop size increased and the surface area of the drops decreased with increasing sodium hydroxide concentration. Sauter mean diameters were 0.082 cm ($A_0 = 0.1$ mol/dm^3), 0.100 cm (0.20 mol/dm^3), and 0.114 cm (0.3 mol/dm^3).

Extraction of *o*- and *m*-Cresol

The results of the extraction of *o*- and *p*-cresol are shown in Fig. 10. It is seen that $C_{I,0}$ influences the y_I vs time relation as in the case of phenol extraction.

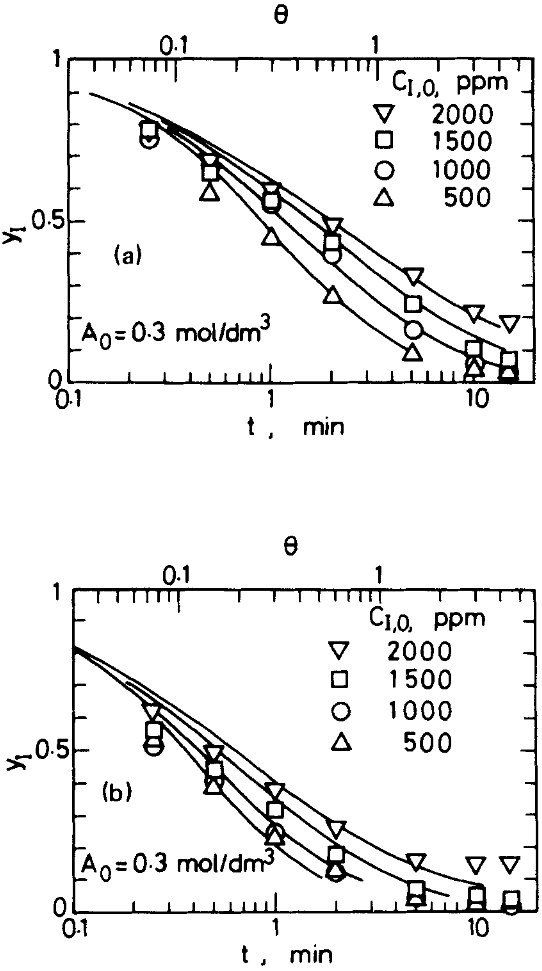

FIG. 8. Effect of the initial concentration of phenol on the y_I vs time relation. Solid lines are the calculated results ($D_e = 1.26 \times 10^{-5}$ cm^2/s, $K_0 = 0.0038$ cm/s). (a) Method A. (b) Method D.

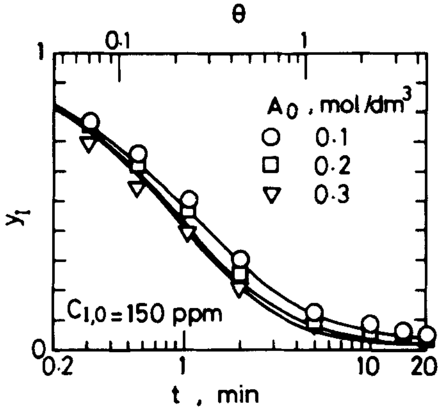

FIG. 9. Effect of NaOH concentration on the extraction rate of phenol. Method B. Solid lines are the calculated results ($D_e = 0.93 \times 10^{-5}$ cm^2/s, $K_0 = 0.0025$ cm/s).

Comparison of y_I after 20 min of Extraction of Phenol with Equilibrium Concentration

The dimensionless equilibrium concentration of phenol, $y_{I,\infty}$, which is the lowest concentration attained when the extraction proceeds ideally without leakage of the internal phase, is given by Eqs. (20) and (21) (*13*):

$$y_{I,\infty} = C_{I,\infty}/C_{I,0} = (-b + \sqrt{b^2 - 4ac})/2a \tag{20}$$

$$\left.\begin{aligned} a &= 1 - \phi' + \phi\phi' + K\phi'(1 - \phi) \\ b &= \phi'[(\phi\beta + \alpha\{\phi + K(1 - \phi)\}] - (1 - \phi')(1 - \alpha) \\ c &= -(1 - \phi')\alpha \end{aligned}\right\} \tag{21}$$

Comparison of $y_{I,\infty}$ with y_I at $t = 20$ min is shown in Fig. 11. As shown by Curve a, $y_{I,\infty}$ decreases with increasing NaOH concentration in the internal phase. However, $y_{I,20}$ shows a minimum when A_0 is 0.3 mol/dm^3. At higher concentrations of NaOH, $y_{I,20}$ increases due to the instability of the oil membrane. It can be seen that the equilibrium concentration increases with increasing initial phenol concentration. Although $y_{I,20}$ is considerably higher than the corresponding value of $y_{I,\infty}$, Curves b and b′ show a similar tendency.

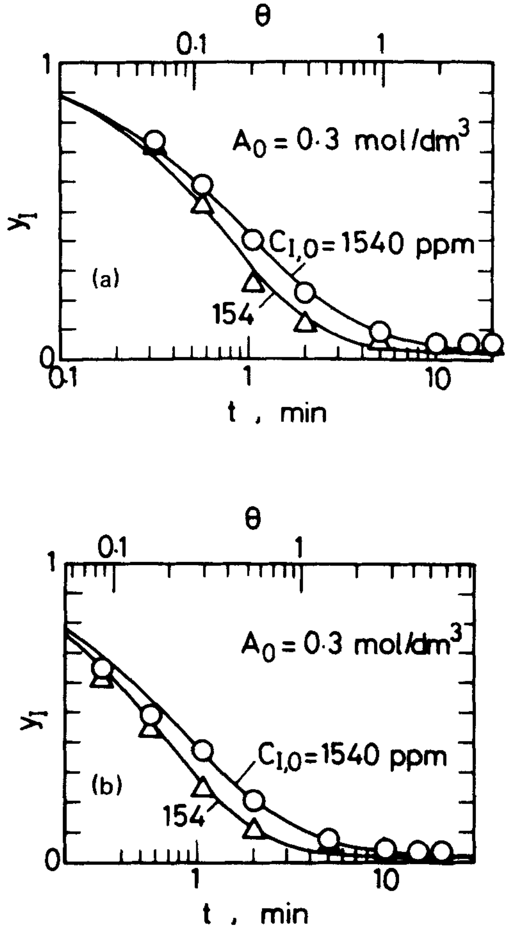

FIG. 10. Extraction of cresol. Method B. Solid lines are calculated results. Parameters are shown in Table 2. (a) *o*-Cresol. (b) *m*-Cresol.

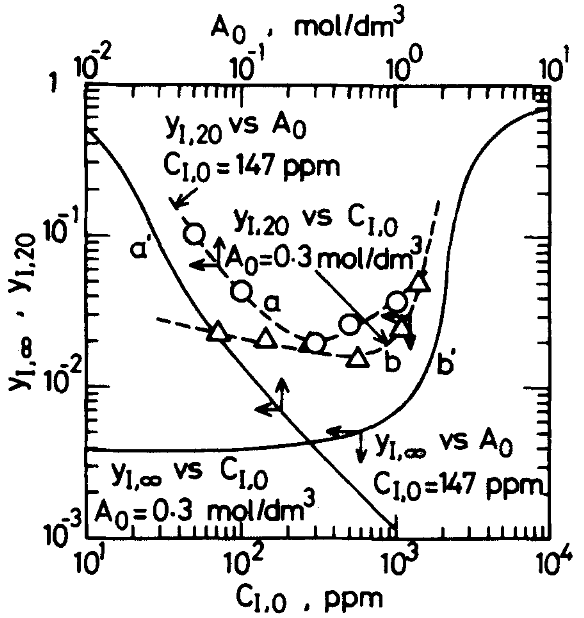

FIG. 11. Comparison of phenol concentration at $t = 20$ min with equilibrium concentration. Method B.

Leakage of Internal Phase to External Phase

The values of f, the fractions of the volume of the internal aqueous phase which leaked to the external aqueous phase due to the breakage of the oil membrane after 15 min of extraction, are listed in Table 1. These are the average values of several experiments. A slightly large value of f was observed in the case of Method D; however, f was relatively small and less than 0.022 under the present experimental conditions.

DISCUSSION

Estimation of Parameters

Of the six parameters involved in the present model, ϕ, ϕ', α, and β can be easily determined from the experimental conditions. K and drop size distribution were measured as described above. Then $Bi_C(=R_CK_0/D_e)$ is the only parameter that must be determined by simulating the experimental data with the present model. This parameter represents the ratio of the internal mass transfer resistance to the overall resistance consisting of the mass transfer resistance through the peripheral layer of the W/O emulsion and the external mass transfer resistance. When Bi_C is small, the latter is rate controlling, and the effect of the initial phenol concentration $C_{\mathrm{I},0}$ on the relation of y_I vs t is small provided that the amount of OH^- in the internal phase is sufficient to keep the equilibrium concentration of phenol considerably low. On the other hand, when Bi_C is large, the internal diffusion is important, and the effect of $C_{\mathrm{I},0}$ is large (*13*). Thus, Bi_C can be estimated so that the computed result may adequately simulate the experimentally observed effect of $C_{\mathrm{I},0}$ on the y_I vs time relation. The solid lines in Figs. 7–10 are the computed relations of y_I vs θ, and these are drawn so that the computed results may fall on the observed relations of y_I vs t by adjusting the position of the upper abscissa with respect to the lower abscissa. To simplify the calculation, the drop size distributions of the W/O emulsion shown in Fig. 5 were also simplified by dividing each of them into 7 portions. The agreement between the computed and the observed results is fairly good. The value of $t_{\theta=1}$ can be read from these figures. Then D_e is calculated by Eq. (22) and K_0 by Eq. (23):

$$D_e = R_c^2/t_{\theta=1} \tag{22}$$

$$K_0 = Bi_C D_e/R_c = Bi_C R_C/t_{\theta=1} \tag{23}$$

The values of $D_{e,\mathrm{exp}}$, D_e thus obtained, are shown in Table 2. The values for the extraction of amines (*13*) are also shown. The values of $D_{e,\mathrm{exp}}$ are in the range from 0.6×10^{-5} to 1.50×10^{-5} cm^2/s, and close to D_II, the diffusivity in the oil phase. To examine whether these values are reasonable, the effective diffusivity in the heterogeneous W/O emulsion, $D_{e,\mathrm{cal}}$ was estimated from the Russel equation (*13, 25*) and is shown in Table 2:

$$E' = \frac{D_e}{D_\mathrm{II}} = \frac{\gamma\phi^{2/3} + 1 - \phi^{2/3}}{\gamma(\phi^{2/3} - \phi) + 1 - \phi^{2/3} + \phi} \tag{24}$$

where $\gamma = D_\mathrm{III}/D_\mathrm{II}K$.

$D_{e,\mathrm{exp}}$ is slightly larger than $D_{e,\mathrm{cal}}$. This discrepancy may be explained as follows. (a) The experimental error in measuring the drop size may have a considerable effect on $D_{e,\mathrm{exp}}$. (b) There is actually some range in Bi_C which is thought to give good agreement between observed and calculated results. (c)

TABLE 2
Summary of Experimental Results

	Phenol	*o*-Cresol	*m*-Cresol	Aniline	*m*-Toluidine	*p*-Toluidine
K^a	1.0	3.5	2.6	1.4	5.3	4.7
pK_a	9.939	10.25	10.09	4.596	4.73	5.08
pK_b				9.404	9.27	8.92
$D_{II} \times 10^5$, cm^2/s^b	1.12	1.00	1.00	1.11	0.993	0.993
$D_{III} \times 10^5$, cm^2/s^b	1.02	0.912	0.912	1.01	0.905	0.905
$D_{e,\mathrm{exp}} \times 10^5$, cm^2/s	0.93–1.26	0.9	1.2	1.20	1.5	0.6
$D_{e,\mathrm{cal}} \times 10^5$, cm^2/s^c	1.06	0.59	0.65	0.91	0.54	0.55
$K_0 \times 10^3$, cm/s	2.5–3.8	3.3	3.3	4.4	3.1	3.5
$y_{I,\infty}{}^d$	0.00687	0.0137	0.00962	0.00203	0.00148	0.000667

[a] Values of K for amines reported in a previous paper (*13*) were the partition coefficients between water and oil in which Span 80 was not contained, and were considerably lower than the values shown in this table.

[b] Diffusivities in oil and aqueous phases were estimated by the Wilke-Chang equation (*27*).

[c] $D_{e,\mathrm{cal}}$ is calculated from Eq. (25).

[d] Values for $C_{I,0} = 0.01$ mol/dm^3 (about 1000 ppm), $[\mathrm{NaOH}]_{III,0}$ or $[\mathrm{HCl}]_{III,0} = 0.3$ mol/dm^3, $\phi = 0.5$, $\phi' = 0.133$, and [Span 80] = 5 vol%.

There may be weak turbulence in the W/O emulsion drop which enhances the mass transfer rate in it. (d) In the internal aqueous phase, phenol can diffuse in the form of either the undissociated species or the dissociated species, i.e., phenolate ion, and the diffusion of phenolate ion may enhance the total mass transfer of phenol in the W/O emulsion drop in the radial direction. Although these phenomena cannot be taken into account in the theoretical analysis, it is clear from the comparison of $D_{e,\mathrm{cal}}$ with $D_{e,\mathrm{exp}}$ that these contributions to the transport of solute in the drop are smaller than that of molecular diffusion.

K_0 is expressed by

$$1/K_0 = 1/k_w + 1/Kk_0 \tag{25}$$

where k_w is the external mass transfer coefficient and k_0 is the mass transfer coefficient through the peripheral layer of the W/O emulsion drop. As shown in Table 2, K_0 is almost independent of partition coefficient K, suggesting that the relation $1/k_w \gg 1/Kk_0$ holds. Then k_w is approximately equal to K_0 in the range from 0.0025 to 0.0044 cm/s. The values agree approximately with the value of k_w, 0.0032 cm/s, estimated using the equation of Calderbank and Moo-Young (*26*).

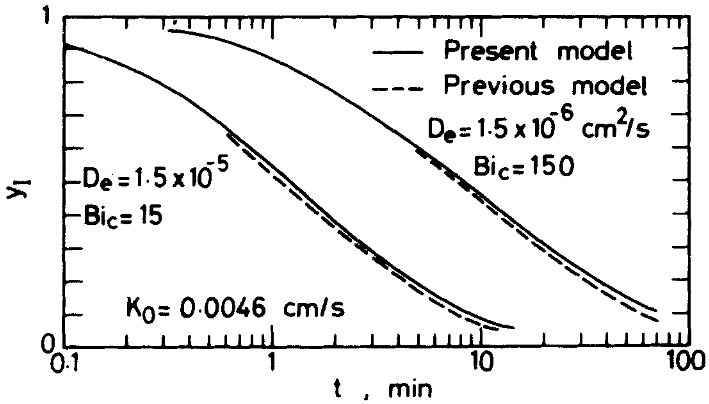

FIG. 12. Comparison of the previous model (*13*) with the present model. $C_{I,0} = 2000$ ppm, $A_0 = 0.3$ mol/dm^3.

Comparison of Previous Model with Present Model

Figure 12 shows a comparison of the results computed from the previous model of the present authors, which assumed uniform drop size distribution (*13*), with those from the present model. The broken lines represent the results from the previous model in which the Sauter mean diameter was used as the average diameter of the drop. As expected theoretically, if Bi_C is small, that is, if mass transfer in the peripheral region of the drop is controlling, the Sauter mean diameter can be used as the average diameter in the previous model. It should be noted, however, that when the amount of OH^- in the internal phase is sufficient so that OH^- except in the peripheral region of the drop may not be consumed, the internal mass transfer resistance is small. In this case, d_{32} can be used as the average diameter even if Bi_C is considerably large. In the early stage of the extraction, the internal resistance is small, and the results computed from both model agree. On the other hand, in the later stages the internal mass transfer becomes important, resulting in slight differences between the computed results.

Simulation of Experimental Data by Complete Mixing Model

The present model can express the various degrees of convection in the W/O emulsion drops by assigning appropriate values to D_e. If considerable convection exists in the drop, there is no mass transfer resistance there, and this situation corresponds to the case of a very small value of Bi_C. Then the basic equations are represented as

$$dy_I/d\tau = -(y_I - y_{II})/(1 - \phi') \tag{26}$$

$$dy_{II}/d\tau = (y_I - y_{II})/[\phi'\{1 - \phi + (\phi/K)g(y_{II})\}] \tag{27}$$

Typical computed results of the above equations are shown in Fig. 13. It is clearly seen that the effect of initial phenol concentration cannot be explained by the complete mixing model.

Comparison of Extraction Rates of Phenol and Aniline

Figure 14 shows the time courses of the extraction of phenol, cresol, aniline, and toluidine. Comparison of the extraction rates of phenol and cresol indicates that cresol is extracted more rapidly than phenol in the early stage of the experiment because K for cresol is much larger than that for phenol. However, in the later stages, the degree of extraction of phenol is higher because of its larger acid dissociation constant, K_a, and lower equilibrium concentration than those of cresol as shown in Table 2. Note that $y_{I,\infty}$ for phenol is lower than for cresol although these values are much smaller than the experimentally observed lowest values of y_I.

It is also indicated that aniline is extracted more rapidly than phenol. One

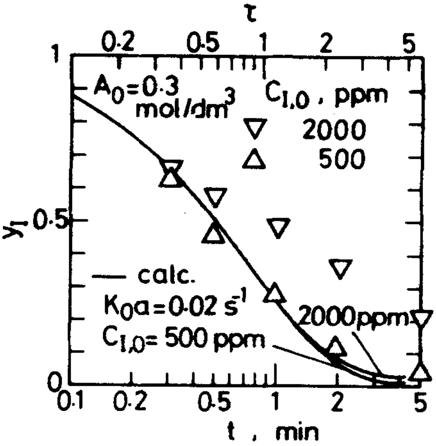

FIG. 13. Simulation of the experimental data by the complete mixing model. Method C.

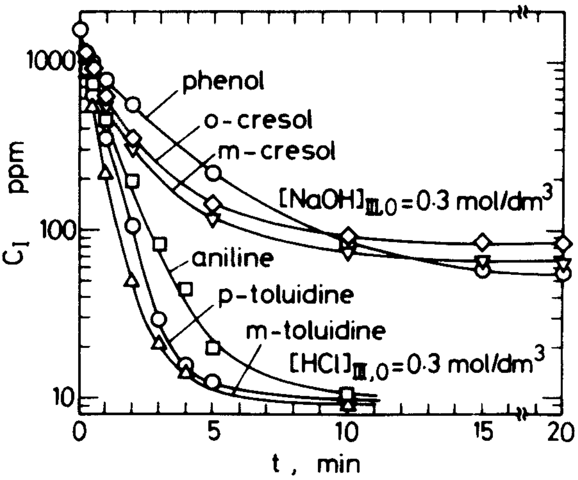

FIG. 14. Comparison of the extraction rates of phenol, cresol, aniline, and toluidine.

of the reasons is that smaller drops were formed in the case of aniline extraction (d_{32} = 0.114 cm for phenol extraction and 0.076 cm for amine extraction). Another reason is that K_b, the base dissociation constant of aniline, which corresponds to K_a for phenol extraction (*13*), is much higher than K_a of phenol, and the extraction of aniline is favorable in view of chemical equilibrium. Toluidine is extracted more rapidly than aniline because the former has higher values of K and K_b.

Recently, Ho et al. (*11*) presented the following equations for evaluating $y_{I,\infty}$ on the basis of a shrinking core model:

$$y_{I,\infty} = (1 - \xi)/(1 + \xi\delta) \tag{28}$$

$$\left.\begin{aligned} \xi &= V_{III}[OH^-]_{III,0}/V_I C_{I,0} = \phi\phi'\beta/(1 - \phi') \\ \delta &= \{\phi + K(1 - \phi)\}/\phi\beta \end{aligned}\right\} \tag{29}$$

Parameter ξ is the initial mole ratio of NaOH in the internal phase to phenol in the external phase. If ξ is greater than unity, $y_{I,\infty}$ becomes negative. This unreasonable result arises because the chemical equilibria are not taken into account in their model. Thus, it should be noted that acid or base dissociation is a very important factor in discussing the rate of extraction as well as the degree of removal.

CONCLUSION

Experimental data on the batch extraction of phenol, *o*-, and *m*-cresol were analyzed on the basis of a model in which the diffusion in the W/O emulsion drop, the external mass transfer around the drop, phase and chemical equilibria, and the drop size distribution were taken into account. The intensity of sonication in the preparation of W/O emulsion was found to have a considerable effect on the properties of W/O emulsion and, in turn, the extraction rate. It was found that the experimental data were satisfactorily explained by the proposed model, and that the acid dissociation constant is an important factor which determines the rate and the extent of extraction. It was also shown that the previous model of the present authors, which assumed uniform drop size distribution of the W/O emulsion, can predict the time course of the extraction if Sauter mean diameter is used as the characteristic diameter of the W/O emulsion drop.

SYMBOLS

A	concentration of OH^- in internal aqueous phase (mol/dm^3)
A_0	initial concentration of OH^- in internal aqueous phase (mol/dm^3)
a	interfacial area between Phase I and W/O emulsion drop per unit volume of W/O/W emulsion (1/cm)
Bi_C	Biot number ($=K_0 R_C/D_e$)
C	concentration of solute (mol/dm^3)
D	molecular diffusivity (cm^2/s)
D_e	effective diffusivity in W/O emulsion drop (cm^2/s)
d_{32}	Sauter mean diameter of W/O emulsion drop (cm)
E	D_e/D_{II}
f	fraction of volume of internal aqueous phase which leaks to external aqueous phase due to membrane breakdown
$g(y_{II})$	function defined by Eq. (17)
K	partition coefficient
K_a	acid dissociation constant (mol/dm^3)
K_b	base dissociation constant (mol/dm^3)
K_0	overall mass transfer coefficient $(1/k_w + 1/Kk_0)^{-1}$(cm/s)
K_w	product of $[H^+]$ and $[OH^-]$ (mol^2/dm^6)
k_0	mass transfer coefficient of peripheral oil layer of W/O emulsion drop (cm/s)

k_w	external mass transfer coefficient around W/O emulsion drop (cm/s)
n_i	number of W/O emulsion drop of radius R_i
P	concentration of phenolate ion (mol/dm^3)
R_C	characteristic radius of W/O emulsion (cm)
R_i	radius of W/O emulsion drop (cm)
r	radial distance (cm)
T	total concentration of phenol ([phenol] + [phenolate ion]) (mol/dm^3)
t	time (s)
V	volume (cm^3 or dm^3)
x	r/R
y_I	$C_I/C_{I,0}$
y_{II}	$C_{II}/KC_{I,0}$

Subscripts

0	initial value
i	value for W/O emulsion drop of radius R_i
I	Phase I (external aqueous phase)
II	Phase II (organic membrane phase)
III	Phase III (internal aqueous phase)
∞	value at equilibrium

Greek

α	$K_a/K_w C_{I,0}$
β	$A_0/C_{I,0}$
γ	D_{III}/KD_{II}
δ	$\{\phi + K(1 - \phi)\}/\phi\beta$
ξ	$V_{III}[OH^-]_{III,0}/V_I C_{I,0} = \phi\phi'\beta/(1 - \phi')$
σ	interfacial tension (N/m)
τ	$K_0 at$
ϕ	volume fraction of Phase III in W/O emulsion ($V_{III}/(V_{II} + V_{III})$)
ϕ'	volume fraction of W/O emulsion in W/O/W emulsion ($V_{II} + V_{III})/(V_I + V_{II} + V_{III})$
θ	$D_e t/R_C^2$

Acknowledgment

This work was partly supported by a Grant-in Aid for Scientific Research from the Ministry of Education, Science and Culture, Japan in 1982 (No. 57030054).

REFERENCES

1. N. N. Li, *AIChE J.*, *17*, 459 (1971).
2. N. N. Li, *Ind. Eng. Chem., Process Des. Dev.*, *10*, 215 (1971).
3. N. D. Shah and T. C. Owens, *Ind. Eng. Chem., Prod. Res. Dev.*, *11*, 58 (1972).
4. R. P. Cahn and N. N. Li, *J. Membrane Sci.*, *1*, 129 (1976).
5. G. Casamatta, C. Chavarie, and H. Angelino, *AIChE J.*, *24*, 945 (1978).
6. P. Alessi, I. Kikic, and M. Orlandini-Visalberghi, *Chem. Eng. J.*, *19*, 221 (1980).
7. W. Halwachs, E. Flaschel, and K. Schügerl, *J. Membrane Sci.*, *6*, 33 (1980).
8. V. J. Kremesec, *Sep. Purif. Methods*, *10*, 117 (1981).
9. N. N. Li and A. L. Shrier, *Recent Developments in Separation Science*, Vol. 1, CRC Press, Boca Raton, Florida, 1972, p. 163.
10. R. P. Cahn and N. N. Li, *Sep Sci.*, *9*, 505 (1974).
11. W. S. Ho, T. A. Hatton, E. N. Lightfoot, and N. N. Li, Paper Presented at the Second World Congress of Chemical Engineering and World Exposition, Montreal, Canada, 1981.
12. T. Kitagawa, Y. Nishikawa, J. W. Frankenfeld, and N. N. Li, *Environ. Sci. Technol.*, *11*, 602 (1977).
13. M. Teramoto, H. Takihana, M. Shibutani, T. Yuasa, Y. Miyake, and H. Teranishi, *J. Chem. Eng. Jpn.*, *14*, 122 (1981).
14. A. M. Hochhauser and E. L. Cussler, AIChE *Symp. Ser.*, 71, 136 (1975).
15. E. S. Matulevicius and N. N. Li, *Sep. Purif. Methods*, *4*, 73 (1975).
16. T. P. Martin and G. A. Davies, *Hydrometallurgy*, *2*, 315 (1976/1977).
17. J. W. Frankenfeld and N. N. Li, *Recent Developments in Separation Science*, Vol. 3, Part B, CRC Press, Boca Raton, Florida, 1977, p. 285.
18. K.-H. Lee, D. F. Evans, and E. L. Cussler, *AIChE J.*, *24*, 860 (1978).
19. W. Völkel, W. Halwachs, and K. Schügerl, *J. Membrane Sci.*, 6, 19 (1980).
20. J. Strzelbicki and W. Charewicz, *Hydrometallurgy*, 5, 243 (1980).
21. J. W. Frankenfeld, R. P. Cahn, and N. N. Li, *Sep. Sci. Technol.*, *16*, 385 (1981).
22. P. Sherman (ed.), *Emulsion Science*, Academic, London, 1968.
23. T. Vermeulen, G. M. Williams, and G. E. Langlois, *Chem. Eng. Prog.*, *51*, 85F (1955).
24. R. Shinnar and J. M. Church, *Ind. Eng. Chem.*, *52*, 253 (1960).
25. H. W. Russel, *J. Am. Ceram. Soc.*, *18*, 1 (1954).
26. P. H. Calderbank and M. B. Moo-Young, *Chem. Eng. Sci.*, *16*, 39 (1961).
27. C. R. Wilke and P. Chang, *AIChE J.*, *1*, 264 (1955).

Received by editor September 8, 1982